



Evolution of cratons through the ages: A time-dependent study

Jyotirmoy Paul^{*}, Attreyee Ghosh

Centre for Earth Sciences, Indian Institute of Science, Bangalore 560012, India

ARTICLE INFO

Article history:

Received 6 June 2019

Received in revised form 28 October 2019

Accepted 7 November 2019

Available online 20 November 2019

Editor: R. Dasgupta

Keywords:

cratons

mantle convection

numerical modeling

study of deep earth interior

ABSTRACT

The viscosity of cratons is key to understanding their long term survival. In this study, we present a time-dependent, full spherical, three dimensional mantle convection model to investigate the evolution of cratons of different viscosities. The models are initiated from 409 Ma and run forward in time till the present-day. We impose a surface velocity boundary condition, derived from plate tectonic reconstruction, to drive mantle convection in our models. Cratons of different viscosities evolve accordingly with the changing velocity field from their original locations. Along with the viscosity of cratons, the viscosity of the asthenosphere also plays an important role in cratons' long term survival. Our results predict that for the long-term survival of cratons they need to be at least 100 times more viscous than their surroundings and the asthenosphere needs to have a viscosity of the order of 10^{20} Pa-s or more.

© 2019 Elsevier B.V. All rights reserved.

1. Introduction

In contrast to the short-lived oceanic lithosphere, which gets recycled every ~ 200 Myrs, cratons have existed for a few billion years. They are the oldest continental lithosphere and some of them are surviving since the Archean with little or almost no deformation since the Cambrian (King, 2005; Pearson et al., 1995; Pearson and Wittig, 2014). In addition to being very old, they also possess a number of unique properties, such as thick lithospheric root (Artemieva and Mooney, 2002; Gung et al., 2003; Polet and Anderson, 1995), neutral density (Jordan, 1975, 1978), low heat flow (Rudnick et al., 1998) and faster seismic velocities (Becker and Boschi, 2002; Ritsema et al., 2011; Simmons et al., 2010; Auer et al., 2014; Garber et al., 2018). It is observed that these long-lived cratons consist of only $\sim 5\%$ of the total surface area of the earth (Hawkesworth et al., 2017). Several studies suggest that $\sim 65-70\%$ of present-day continental volume was already produced before ~ 3 Ga but underwent extensive deformation and recycling, leaving this $\sim 5\%$ of "patchy" rock records as cratons (Hawkesworth and Kemp, 2006; Hawkesworth et al., 2017; Dhuime et al., 2012; Belousova et al., 2010). Although in a few cases, cratons might have been destroyed (e.g., North China (Zhu et al., 2012)), traditionally cratons have survived for a long time against convective forces in the mantle. It certainly raises an important question that in spite of extensive deformation during the Archean-Proterozoic time, how did these cratons and their thick roots survive.

To address the long term survival of cratons, earlier studies have proposed that cratons are made up of a compositionally buoyant continental lithosphere compared to its surroundings and thus remain unaffected by subduction (Jordan, 1975, 1978). In his basalt depletion hypothesis, Jordan (1978) advocated that removal of basaltic melt from garnet lherzolitic mantle composition left a less dense residue as continental lithosphere, which became gravitationally stable and emerged as stable cratons. It is possible that such neutrally buoyant continental lithosphere may avoid gravitational delamination, however, they need to achieve tectonic stability (Foley, 2008; Lenardic et al., 2003) against the convective forces exerted by the viscous mantle. An example is western North America, where in spite of significant tectonic modifications along the western margin, the adjacent cratons' interiors have remained unaffected (cf. Hoffman (1988)), except for a few cases such as the Wyoming craton (e.g. Humphreys et al. (2015)). Several studies have suggested that such tectonic inertness of cratons can only be achieved if they are strong enough to resist the mantle convection forces (Lenardic and Moresi, 1999; Lenardic et al., 2003; Wang et al., 2014; O'Neill et al., 2008; Cooper et al., 2004; Lee et al., 2005, 2011; Yoshida, 2012, 2010).

Importance of material strength in the survival of cratons was emphasized by Pollack (1986). He claimed that a higher degree of partial melting during the hotter Archean environment led to the devolatilization of cratonic roots. This would have eventually made them highly viscous along with maintaining their freeboard achieved by chemical depletion (Jordan, 1978). Determination of the viscosity of cratons has remained elusive. Although real samples of cratonic roots are available as mantle xenoliths, mineral physics studies are unable to determine the precise viscosity of the

^{*} Corresponding author.

E-mail address: jyotirmoy@iisc.ac.in (J. Paul).

xenoliths. The reasons range from experiments being conducted on single phase minerals rather than complex rocks to laboratory studies that are limited to a much shorter time period compared to geological time scale as well as the influence of water and pressure (Karato, 2010). Numerical modeling offers another possible way of estimating the viscosity of cratonic materials. Lenardic and Moresi (1999) developed simple 2-D models and showed that possessing only neutral density cannot make the cratons tectonically stable. Cratons' roots need to be highly viscous in order to resist the convective forces. Using further sophisticated 2-D models, Lenardic et al. (2003) showed that a cratonic root of 120 km thickness having a density of 3200 kg/m^3 (lower than mantle peridotite density of 3300 kg/m^3) became unstable within 70 Myrs, provided no viscosity contrast was applied to the cratonic root. However, when cratonic roots were strengthened with 1000 times higher viscosity than the surroundings, they remained stable for a much longer time within the same models (Lenardic et al., 2003). O'Neill et al. (2008) also developed 2-D models and estimated that the viscosity contrast between cratons and the surrounding asthenosphere should be 50-150 provided the yield strength ratio between cratonic roots and oceanic lithosphere is 5-30. Recently, using non-Newtonian viscosity in their 2-D models, Wang et al. (2014) observed that a very small viscosity contrast of order 10 can resist the cratonic roots against small scale convective erosion for more than 2 billion years irrespective of whether the root is buoyant or not. They concluded that the density of cratonic roots plays a secondary role in their survival whereas the viscosity of the cratons is the primary factor. Kaban et al. (2015) constructed a 3-D compositional density model of North America by inverting residual gravity field and residual topography and showed that the compositionally depleted root of the North American craton is deforming at a faster rate than the rest of the craton, indicating that a compositionally buoyant root is more prone to deformation. All these studies more or less conclude that the material strength of cratons is fundamental for their survival.

The above studies addressed the issue of survival of cratons using 2-D models. Yoshida (2010) constructed the first 3-D spherical models of evolution of continental lithosphere in a restricted regional domain to address the deformation within the cratons. Yoshida (2012) also used 3-D models to investigate the contribution of weak continental margins in protecting the cratonic lithosphere. He quantitatively estimated that a viscosity contrast of the order of 10^6 between weak continental margins and cratonic lithosphere can increase the longevity of cratonic lithosphere. The concept of weaker zones protecting the cratons was also tested in 2-D models by Lenardic et al. (2000) and Lenardic et al. (2003).

To address the issue of cratonic survival, Paul et al. (2019) developed 3-D earth-like full spherical instantaneous mantle convection models with lateral viscosity variations, in which they used density anomalies inferred from present-day tomography to drive flow. They quantified the amount of mantle shearing at the variable base of the lithosphere and the corresponding strain-rates. Their results showed that the intensity of deformation at the base of the lithosphere decreases with increasing lithosphere thickness. Hence, although the cratons experience higher tractions at their bases compared to other types of lithosphere (e.g. oceanic or non-cratonic continental lithosphere), they could potentially survive for a long time because of low strain-rates. They also inferred that a combination of asthenosphere viscosity no less than 10^{20} Pa-s and cratonic roots at least 100 times more viscous compared to their surroundings can potentially give rise to stable cratons.

In the present study, we try to understand the reasons of cratonic survival using 3-D, full, spherical mantle convection models similar to Paul et al. (2019). The difference is that while Paul et al. (2019) used instantaneous models driven by density anomalies obtained from tomography, the current study uses time-dependent

convection models using reconstructed surface velocities as the driver of mantle convection. Our motivation is to observe how cratons of different viscosities evolve over time under the influence of convective shearing exerted by mantle flow. We also seek to investigate whether asthenosphere viscosity has any significant role to play in cratons' survival. Some of the earlier studies, e.g. Conrad and Lithgow-Bertelloni (2006), had suggested that the asthenosphere has a negligible role to play in affecting the tractions at the base of the lithosphere, whereas Paul et al. (2019) suggested a significant contribution of asthenospheric viscosity to cratonic survival. Along with observing the evolution and subsequent deformation pattern of the cratons, in the current study we also test the estimates of viscosity combination of asthenosphere and cratons provided by Paul et al. (2019) in their instantaneous models that enable the long-term survival of cratons.

2. Methodology

2.1. Mantle convection model

We construct 3-D, spherical, time-dependent global mantle flow models using the finite element code CitcomS (Zhong et al., 2000) that can solve the standard thermal convection equations taking into account conservation of mass, momentum and energy assuming Boussinesq approximation and infinite Prandtl number. This code assumes mantle to be a viscous and incompressible spherical shell. It divides the mantle into 12 topological caps and finite element calculations are operated on each node inside these caps. We create $65 \times 65 \times 65$ nodes in each topological cap that generate outputs at an average horizontal resolution of 1×1 degree. Vertical outputs are generated at 24 km intervals in the top 300 km of the mantle and below that, they are generated at 50 km intervals down to the core-mantle boundary.

Our time-dependent model is developed using plate driven flow in a Newtonian viscous model. Such kind of time-dependent studies spanning more than 400 Myrs using plate reconstruction models are not very common with a few exceptions, such as Zhang et al. (2010) that modeled the evolution of mantle structure for the last 450 Myrs. Presently, we initiate our models at 409 Ma by prescribing surface velocities obtained from GPlates (Boyden et al., 2011; Gurnis et al., 2012) that act as the driver of mantle flow. We update the velocity field at every 1 Myr for the next 410 Myrs. Because of large uncertainties in the density structure of the earth's mantle since 409 Ma, we have not included any density anomaly in our convection models. This affects plate-boundary strain-rates slightly, however, plate interior dynamics are not significantly influenced. We have kept the core-mantle boundary at free-slip condition. A Rayleigh number of 4.4×10^8 is assigned in all the models with a temperature difference of 1300 K (cf. Ghosh et al., 2010, 2013, 2017) between the surface and the core-mantle boundary. Values of thermal diffusivity and coefficient of thermal expansion in our models are $10^{-6} \text{ m}^2/\text{s}$ and $3 \times 10^{-5} \text{ K}^{-1}$ respectively.

2.2. Reconstruction of cratons and surface velocity

GPlates (Boyden et al., 2011; Gurnis et al., 2012), an open source software, can reconstruct any location on present-day earth's surface using the finite rotation of Euler poles. We have chosen a continuous plate reconstruction model by Matthews et al. (2016), which can reconstruct the locations of cratons until 410 Ma (some new models can predict till 1000 Ma, however, those are still under construction for GPlates usage on a global scale). This paleo-reconstruction model is a combination of two earlier models by Domeier and Torsvik (2014) for the time period of 410-250 Ma and Müller et al. (2016) for 230-0 Ma, with adequate modifications ensuring the continuity between 230-250 Ma. The model provides

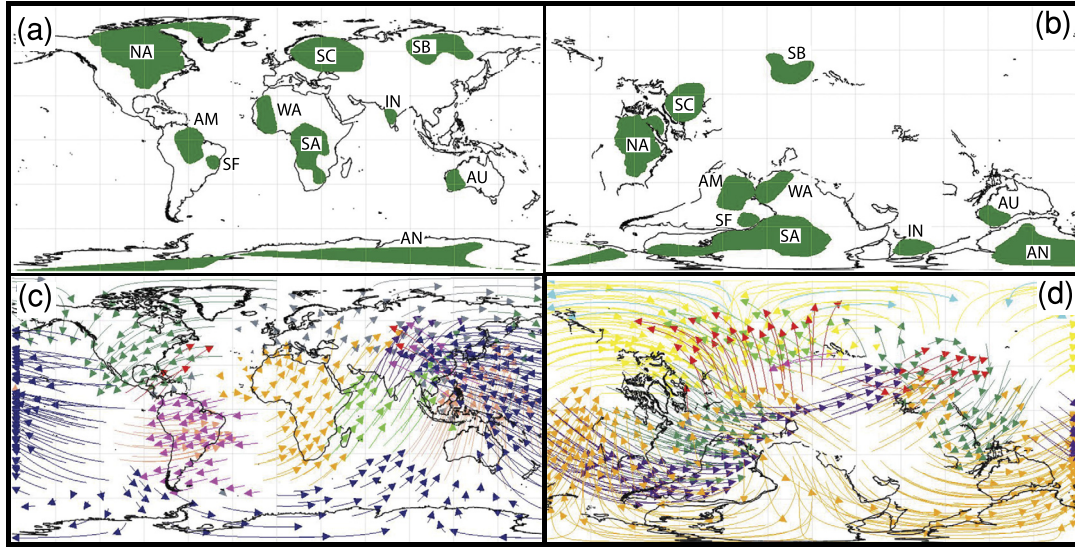


Fig. 1. Location of cratons at the present-day (a) and at 409 Ma (b) marked by green. The cratons are, AN: Antarctica, AM: Amazonian, AU: Australia, IN: India, NA: North America, SA: South Africa, SB: Siberia, SC: Scandinavia, SF: Sao Fransisco, WA: West Africa. Reconstruction of cratons' locations is achieved using the finite rotation of Euler poles in Gplates. Plate velocity at present-day (c) and at 409 Ma (d) are represented by arrows. The arrow colors represent velocity in different topological caps obtained from GPlates.

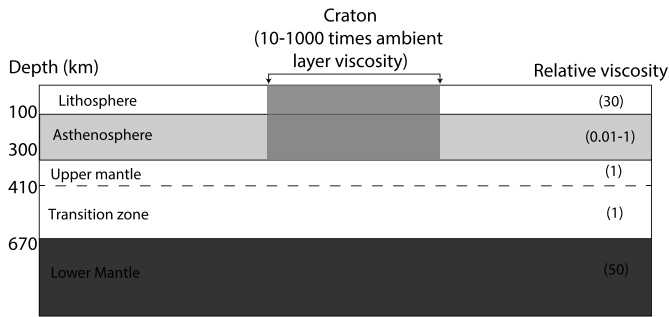


Fig. 2. Schematic diagram of the viscosity structure of the lithosphere and mantle that is considered in our models. Reference upper mantle viscosity is 10^{21} Pa-s. Relative viscosities (mentioned within brackets) of the layers are multiplied by the reference viscosity to obtain the absolute viscosity of the layers. Viscous cratons are incorporated till 300 km depth. The prescribed velocity boundary condition is imposed on the top surface of the model domain and the bottom surface (2891 km) is kept at free-slip condition.

continuously evolving plate boundaries at 1 Myr time interval. We have chosen present-day locations of Archean cratons from 3SMAC model (Nataf and Ricard, 1996) and have reconstructed their locations at 409 Ma using GPlates assuming cratons to be rigid bodies (Fig. 1a, b). Additionally, the plate velocities calculated by GPlates from the finite rotation of Euler poles are imposed as kinematic boundary condition at the surface to drive mantle convection in our models (Fig. 1c, d).

2.3. Mantle viscosity structure

We have followed the approach of Conrad and Lithgow-Bertelloni (2006) to develop the radial viscosity structure of the mantle. The mantle is divided into 5 layers of different viscosities (Fig. 2). Top 100 km is lithosphere with relative viscosity of 30, i.e., it is 30 times stronger than the reference upper mantle viscosity (10^{21} Pa-s). The lithosphere is followed by a weaker asthenosphere (100 - 300 km), upper mantle (300 - 410 km), transition zone having the same viscosity as the upper mantle (410 - 660 km) and strongest lower mantle (660 - Core-Mantle Boundary) with a relative viscosity of 50. In our models, asthenosphere viscosity varies from 0.01 to 1 times the reference mantle viscosity.

We employ lateral viscosity variations on top of the radially varying viscosity structure by incorporating highly viscous cratons as tracers in the models. Two traces are used in our models: one for cratonic areas and the other for non-cratonic areas. We have provided the initial location of cratons at 409 Ma (Fig. 1b) and have made them 300 km thick. Viscosity of cratons is varied between 10 and 1000 times their ambient layer viscosity. For example, cratonic viscosity multiple of 10 will have an actual viscosity of 3×10^{23} Pa-s in the top 100 km and 10^{22} Pa-s in the asthenosphere if the asthenosphere viscosity is 10^{21} Pa-s. A detailed description of viscosity parameters is given in Table S1. As there is no temperature anomaly, the viscosity of cratons is not further modified by temperature dependent viscosity. However, during their evolution for 410 Myrs, the craton viscosity gets modified. Thus with three different asthenospheric viscosities and three different craton viscosities, we produce nine models of all possible viscosity combinations. Once convection begins, cratons start evolving guided by the mantle flow. Depending on their viscosities, cratons get deformed in the time-dependent forward convection models.

3. Evolution of cratons through time

3.1. Survival of cratons till the present-day

Viscous mantle flow exerts tractions at the base of the lithosphere that lead to deformation. Being thick and highly viscous, cratonic lithosphere experiences a unique deformation pattern throughout its evolution in the mantle convection models. We initiate our models at 409 Ma and cratons of different viscosities evolve under the action of mantle flow up to the present-day. Although CitcomS can produce output in time intervals of ~ 0.1 Myr, because of the large volume of data that is produced, we save outputs at $\sim 5 - 10$ Myr time intervals. Hence, often the time nearest to the present-day is at 8 - 5 Ma, else the models overrun up to some future time. The evolution of the models is shown in maps where the cratons can be identified by their higher viscosities (Figs. 3-7). Unlike Yoshida (2012), who looked at the deformation pattern of the continental lithosphere only at the surface, we look into how cratons are deforming at different depths. However, we pay more attention to the deformation patterns at depths greater

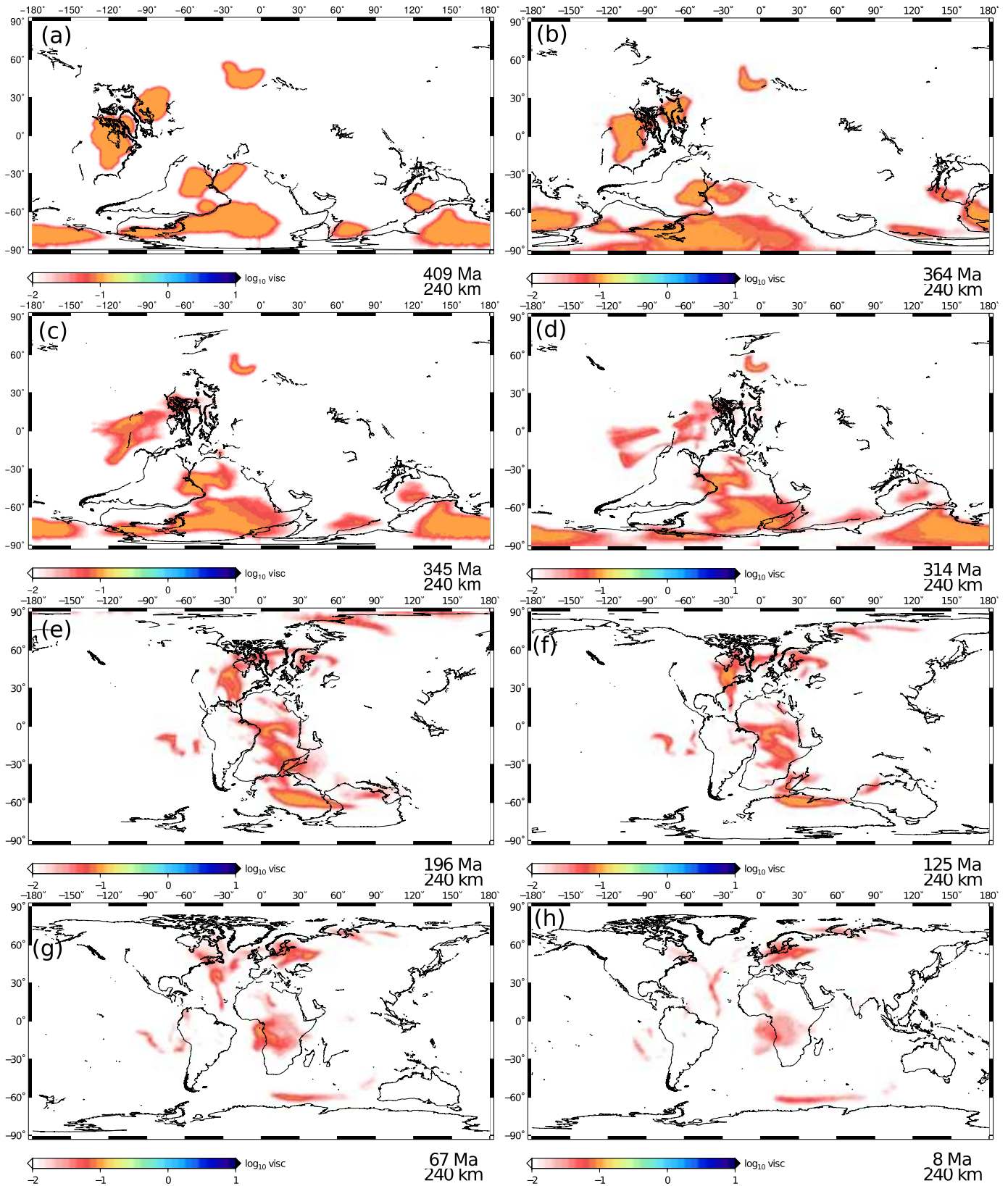


Fig. 3. Evolution of cratons at 240 km depth. Asthenosphere viscosity is 10^{19} Pa-s, cratons are 10 times stronger than surroundings (0.01, 10).

than 200 km, which correspond to the depths of cratonic roots. The survival potential of cratons could be estimated by observing how the roots deform over time (Lenardic et al., 2003; Wang et al., 2014).

The weakest model in terms of viscosity combinations includes an asthenosphere viscosity of 10^{19} Pa-s with cratons 10 times more viscous (0.01, 10) compared to their surroundings (Figs. 3, 4, V1). In this case, at 240 km depth, cratonic roots start to

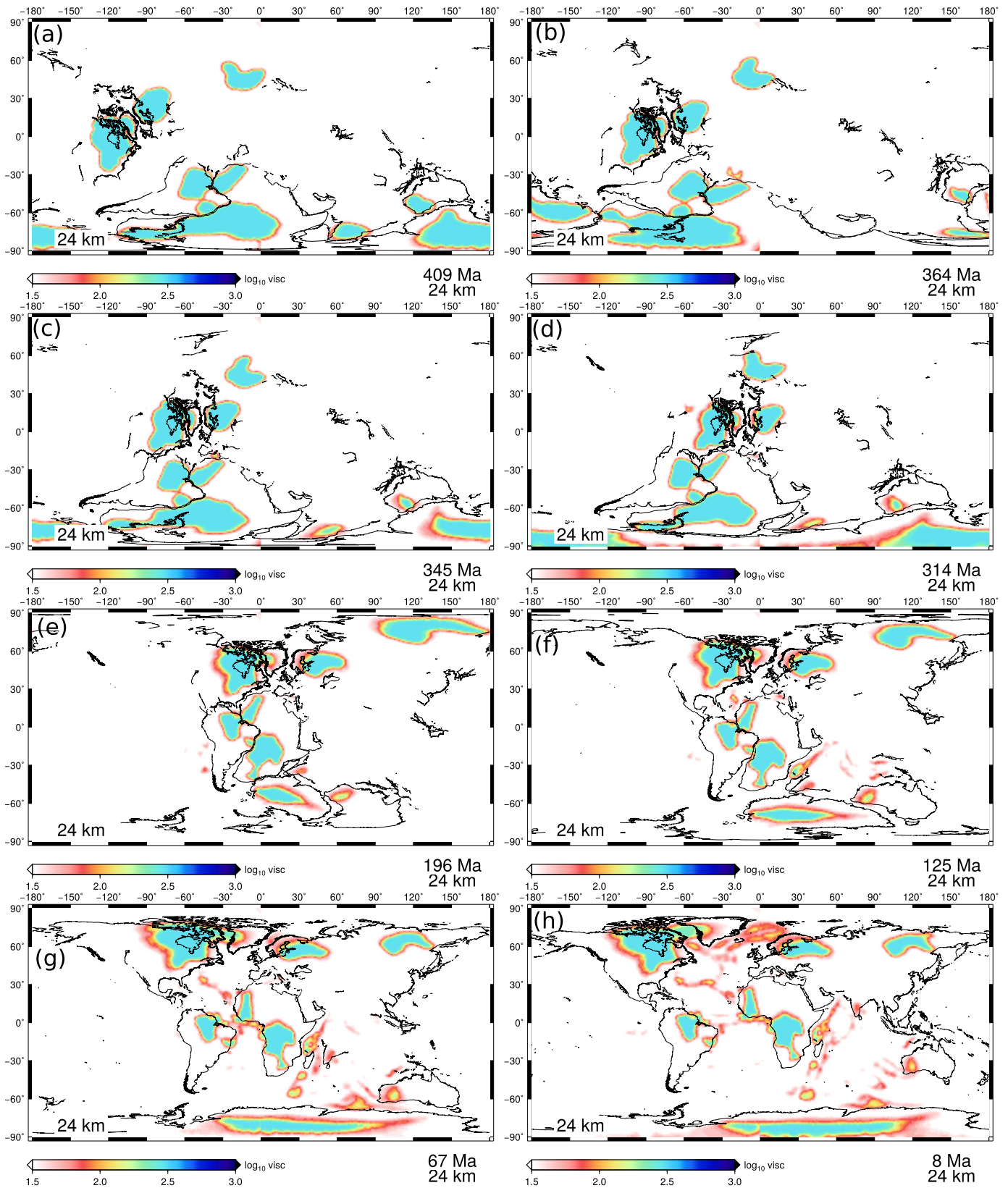


Fig. 4. Evolution of cratons at 24 km depth. Asthenosphere viscosity is 10^{19} Pa-s, cratons are 10 times stronger than surroundings (0.01, 10).

deform significantly within the first 50 Myr (Figs. 3a, b). During the Pangea supercontinent formation ($\sim 350 - 300$ Ma), cratons do not seem to have amalgamated to make a single unit (Figs. 3c, d). Additionally, during the break-up of the supercon-

tinent ($\sim 200 - 170$ Ma), cratonic roots are vigorously destroyed (Fig. 3e). By the time they reach the present-day, cratonic roots at more than 200 km become almost non-existent (Figs. 3g-h, S1). This observation matches with the results obtained from 2-D mod-

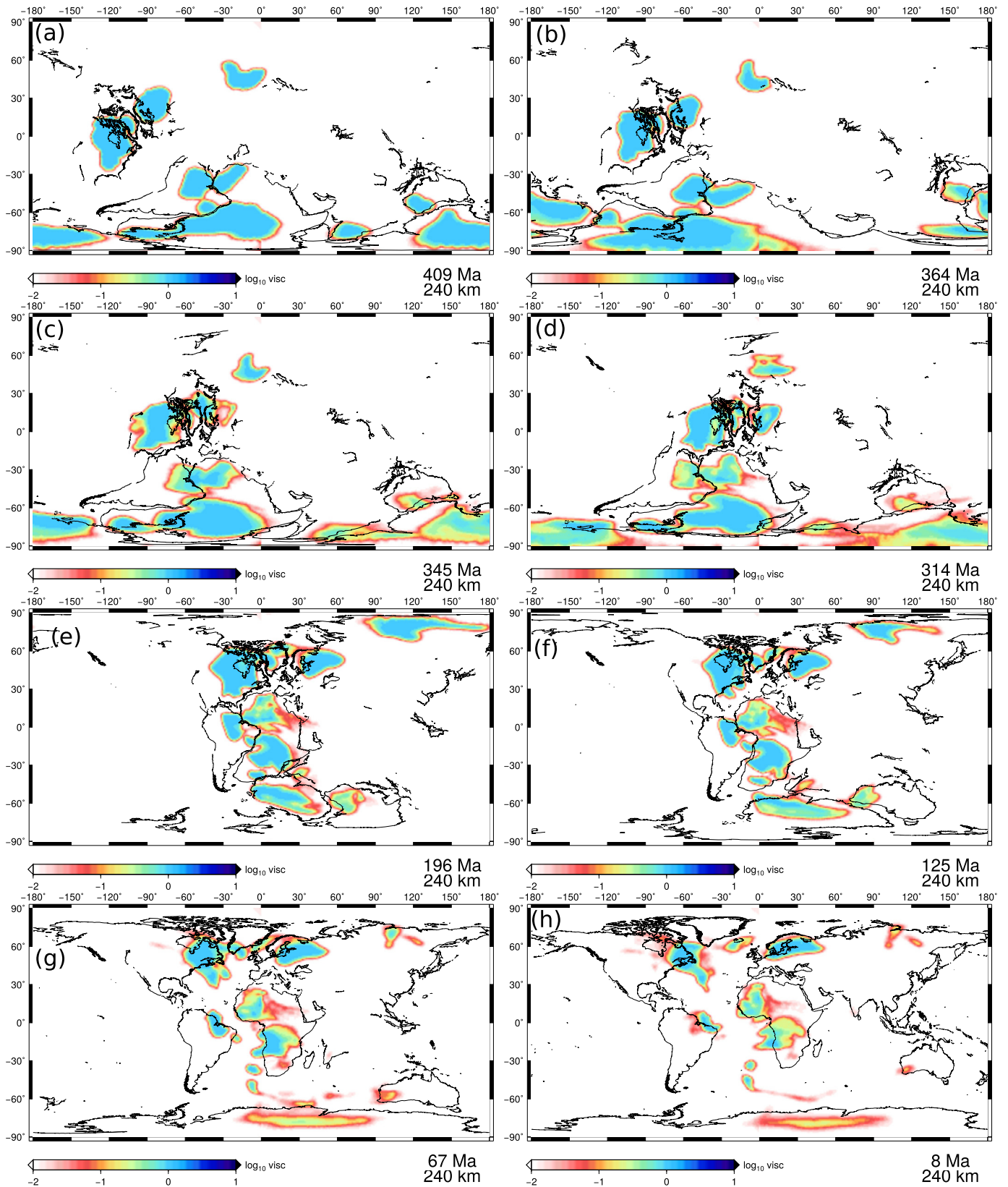


Fig. 5. Evolution of cratons at 240 km depth. Asthenosphere viscosity is 10^{19} Pa-s, cratons are 100 times stronger than surroundings (0.01, 100).

els of Lenardic et al. (2003) and Wang et al. (2014), who showed that cratons get destroyed by shortening their roots. Near the surface also (at shallower depth), cratons seem to deform significantly (Fig. 4). Till the formation of the supercontinent ($\sim 350 - 300$ Ma),

their shapes near the surface are more or less intact (Figs. 4a-d). After the continental breakup starts ($\sim 200 - 180$ Ma), cratons start to deform rapidly near the surface (Figs. 4e-h, 8, S2) by stretching or expansion of cratonic area. Such enhanced surface

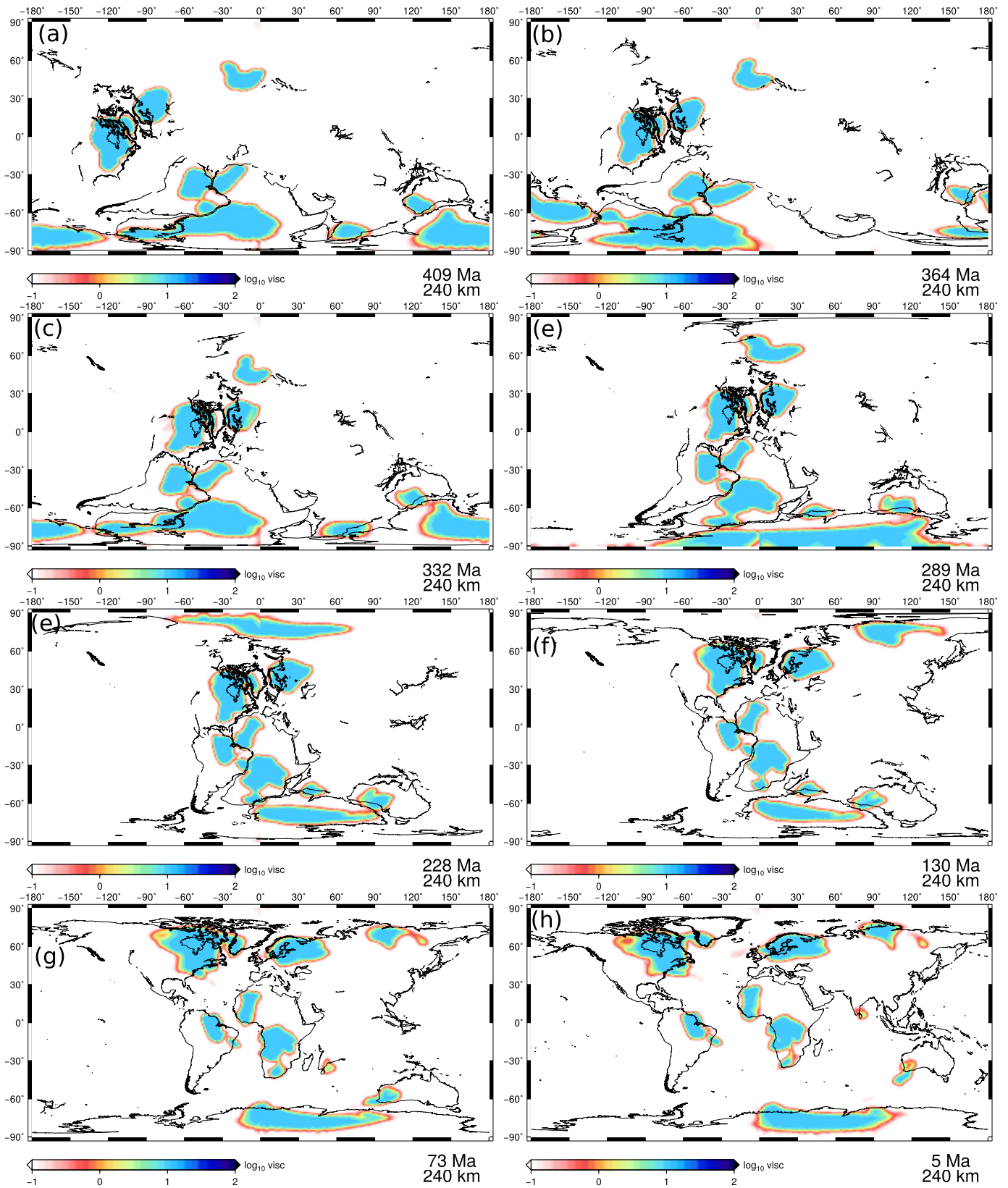


Fig. 6. Evolution of cratons at 240 km depth. Asthenosphere viscosity is 10^{20} Pa-s, cratons are 100 times stronger than surroundings (0.1, 100).

extension of cratons is observed particularly after the opening of the North Atlantic ocean (~ 140 Ma) and during the final stage of the Pangea break-up in the late Cretaceous and early Cenozoic ($\sim 100 - 60$ Ma, Fig. 8d, e). This observation is in agree-

ment with Yoshida (2012) who commented on the deformation of cratons by looking at the stretching of the continental lithosphere at the surface. Except for his stable model, which was surrounded by very weak continental margins, all other mod-

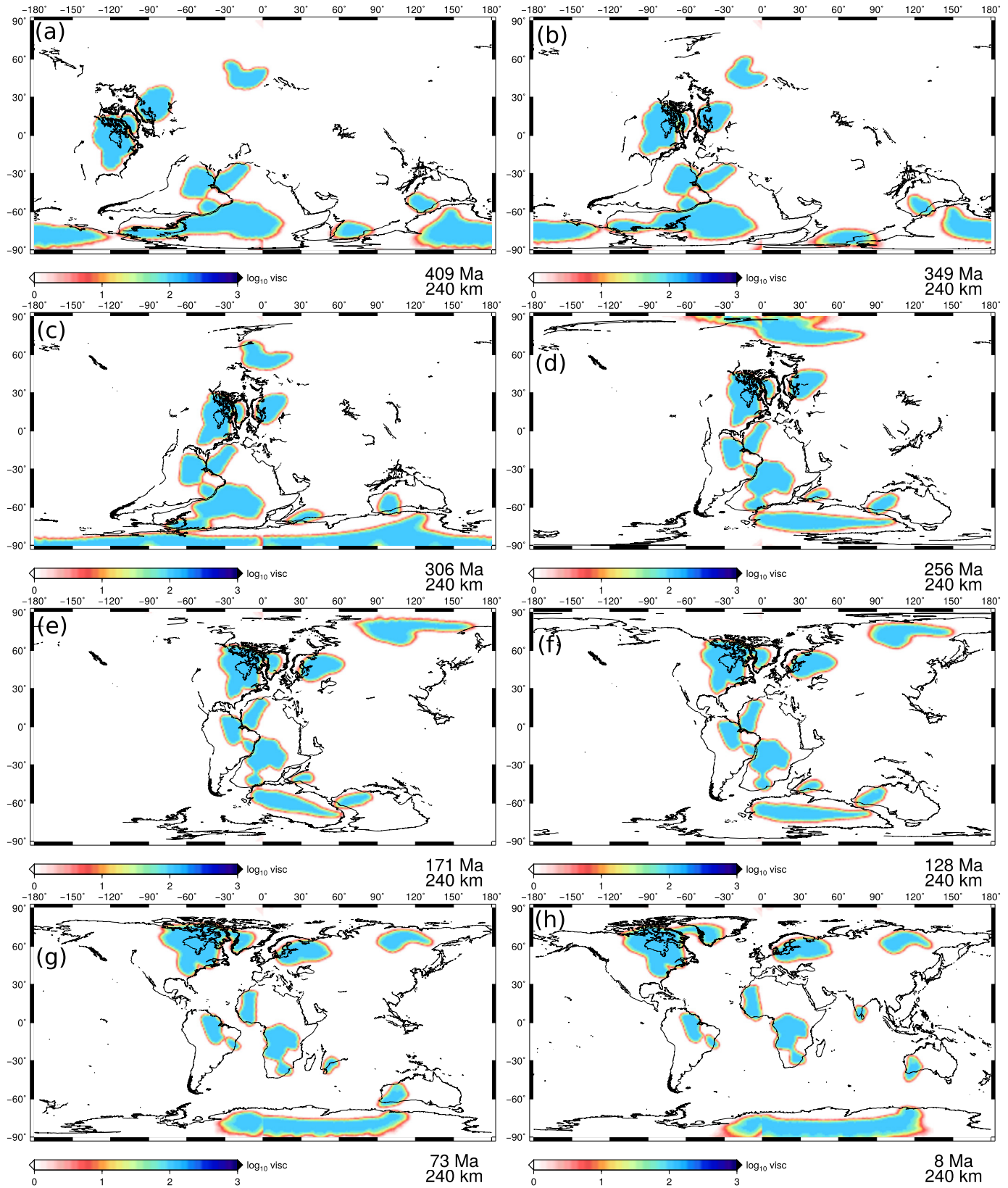


Fig. 7. Evolution of cratons at 240 km depth. Asthenosphere viscosity is 10^{21} Pa-s, cratons are 100 times stronger than surroundings (1, 100).

els showed large stretching of cratonic surface area as time progressed.

Increasing the viscosity of cratons by one order of magnitude to 100, and keeping the asthenosphere viscosity same as 10^{19} Pa-s

(0.01, 100), changes the deformation pattern of cratons (Figs. 5, 8, V2). Deformation of cratonic roots in the first 50 Myr (~ 360 Ma) is not significant (Fig. 5a, b). During the supercontinent formation ($\sim 350 - 300$ Ma), all the cratonic roots clump together

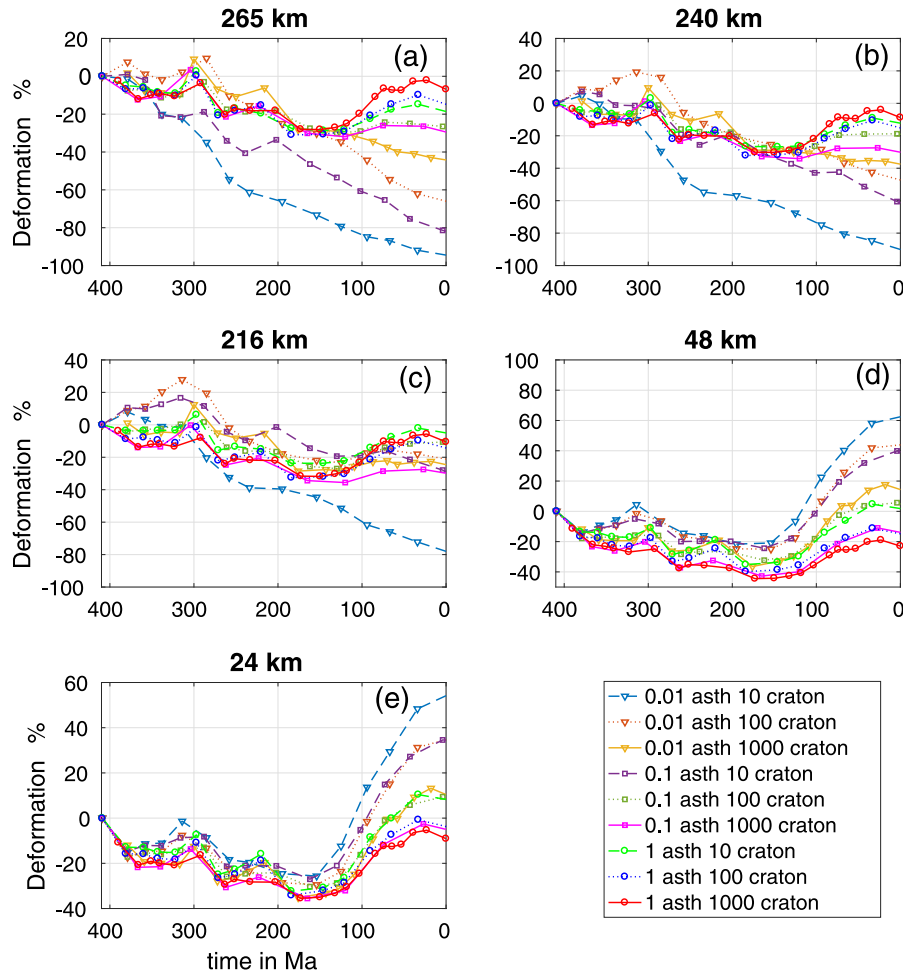


Fig. 8. Areal deformation of cratons at different depths are plotted against time. Each line represents the areal deformation obtained from different asthenosphere and craton viscosity combinations.

to form a larger mass (Fig. 5c, d). During and after the breakup of Pangea (beginning at ~ 200 Ma), cratonic roots start to disintegrate and deform rapidly (Fig. 5e-f), however, this deformation is relatively less than the earlier model (Fig. 3). After ~ 400 Myr, cratonic roots are heavily deformed, although some of the root cores still remain (Figs. 5h, S1). It is to be noted that smaller cratons (e.g. India, Sao Francisco) completely lose their roots, whereas, roots of larger cratons are significantly reduced and deformed. Similar kind of surface stretching of cratonic lithosphere as in the earlier case (Fig. 4) is also observed in this case (Figs. 8, S2).

When we consider the case where the viscosity of the asthenosphere is increased by one order of magnitude (10^{20} Pa-s) compared to the weakest case and cratons are kept as 100 times more viscous relative to their surroundings (0.1, 100; Fig. 6, V3), viscosity maps show that deformation of cratonic roots has slowed down significantly. There is almost no visible deformation of the cratonic roots in the first 50 Myr (Fig. 6a, b). All the edges of cratonic roots have remained sharp. In between 350-200 Ma, all the cratonic roots come together to create a supercontinent (Fig. 6c-e) and after the breakup of the supercontinent, they retain their shapes till ~ 100 Ma (Fig. 6f, g). As time progresses, roots experience more deformation and their shapes gradually evolve. At ~ 5 Ma (Fig. 6h) it can be seen that the North American, Amazonian and Siberian cratonic roots are slightly stretched along NW-SE direction, while the Australian craton and part of the South African craton are stretched along NE-SW direction. Small disintegration is observed near the Scandinavian craton and the root under the

Indian craton is reduced in size. In spite of the overall deformation, the final shape of all the cratons obtained from this model is comparable to the shape of present-day cratons (Figs. S1, S2).

Keeping the cratons 100 times more viscous than their surroundings and increasing the viscosity of asthenosphere to 10^{21} Pa-s (1, 100) reduces the deformation of cratons significantly (Figs. 7, 8, V4). After ~ 400 Myrs, cratons not only remain mostly undeformed but also reach the present-day locations (Figs. 7h, S1, S2). Formation and break-up of the supercontinents have negligible effect on the cratons' evolution pattern. Even smaller cratons like India and Sao Francisco remain undeformed.

3.2. Areal deformation of cratons

In this section, we present a quantitative analysis of how cratons have deformed with time. The precise estimate of the intensity of deformation is quite complicated as we observe different modes of deformation occurring within the cratons. One way to deform the cratons is erosion along the craton boundaries and the other is stretching followed by further disintegration of the cratons (Fig. 9). Combination of all these processes is manifested in the change of cratonic areas. Hence, net areal deformation (D) will be given as $e + s + d_e$, where e is the erosion along the craton boundary, s is the surface stretching of cratons and d_e is disintegration. Erosion (e) will always reduce the cratonic area whereas stretching (s) will always increase it. Disintegration may or may not affect the total surface area. However, if the smaller disintegrated pieces are extremely weak they can easily be eroded by

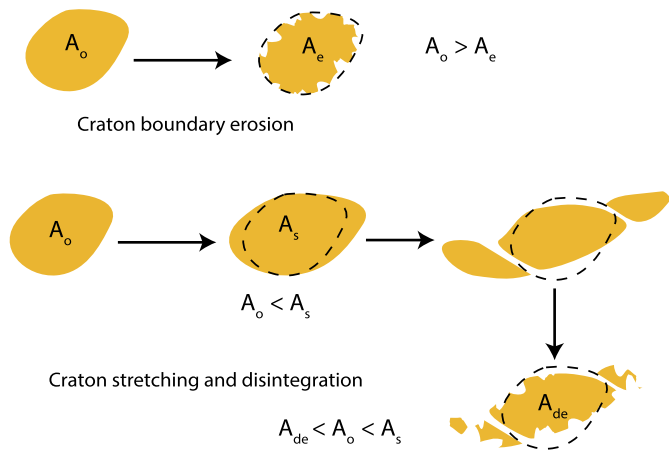


Fig. 9. Schematic diagram of the mode of craton deformation. In the craton boundary erosion, initial craton area A_o is reduced to A_e , while during stretching, initial craton area A_o is increased to A_s . With further stretching, it leads to disintegration and erosion of smaller areas resulting in the reduction of the total area to A_{de} .

the surrounding flow. Such a phenomenon will reduce the area and we quantify this as d_e . Which mode of deformation will dominate during the cratonic evolution will depend on the viscosity of cratons and asthenosphere and the induced velocity field at the surface.

To quantify the net deformation, we calculate the areal change of cratons as: $D = \frac{A_{d,409} - A_{d,t}}{A_{d,409}} \times 100$. Here, $A_{d,409}$ is the area of craton at a certain depth d at 409 Ma and $A_{d,t}$ is the area of craton at depth d and time t . Areal deformation of cratons at different depths are plotted against time (Fig. 8). If the erosion along the craton boundaries dominates, which is clearly observed for weaker cratons (Figs. 3, 5), the net cratonic area is reduced. It is to be noted that such areal reduction is not monotonic as it is also often affected by stretching that tends to increase the area of the cratons, which is likely to be a result of asthenosphere and craton viscosity. Stretching can lead to disintegration of cratonic materials and eventually further reduction in the net area. If weak cratons are surrounded by weak asthenosphere, both the processes of erosion and disintegration can occur simultaneously and destroy the roots quickly. Such a pattern is extensively visible in map views of cratonic evolution (Figs. 3, 5). If the viscosity of the material surrounding the cratons increases, it slows down the disintegration process. Hence, the cratons may undergo stretching, however, they may not completely disintegrate (Fig. 4). It is likely that near the surface, where cratons are surrounded by stronger lithosphere, they experience significant stretching, but do not completely disintegrate like their roots. If the viscosity of cratons and asthenosphere is increased, stretching diminishes, and erosion along the craton boundaries becomes the dominant mode of deformation. If the asthenosphere viscosity is more than 10^{20} Pa-s and cratons are 100 times more viscous than surroundings, the effect of stretching is almost negligible in the net deformation (Figs. 6, 7).

Cratonic roots in the weakest model (0.01, 10) reduce their area by $> 90\%$ within 400 Myr (Fig. 8a, b, c) while they undergo stretching by $\sim 60\%$ close to the surface (Fig. 8d, e). Such a large reduction in root area along with intense surface stretching indicate that with this particular viscosity combination of asthenosphere and cratons (0.01, 10), cratons will not be able to survive for ~ 410 Ma. This is also substantiated by the viscosity maps, where it is clear that the cratonic roots are completely destroyed after ~ 400 Myr (Fig. 3). Cratons that are 10 times more viscous than the previous case and surrounded by asthenosphere of 10^{19} Pa-s viscosity (0.01, 100) undergo $\sim 20 - 70\%$ areal reduction of roots (Fig. 8a, b, c). Additionally, their surface stretching is more

than 40% (Fig. 8d, e). Such a viscosity combination (0.01, 100), is thus unlikely to be suitable for long term survival of cratons, however, they are able to marginally survive for ~ 410 Myr (Fig. 5). Within a similarly weak asthenosphere of viscosity 10^{19} Pa-s, if cratonic roots become 1000 times more viscous (0.01, 1000), their root deformation is restricted within $\sim 20 - 40\%$ (Fig. 8a, b, c) and surface stretching is limited within $\sim 20\%$ (Fig. 8d, e). Such a viscosity combination (0.01, 1000) can possibly increase the survival time of cratons compared to the previous case. However, their long term survival of more than 2 billion years remains questionable.

If the asthenospheric viscosity is taken as 10^{20} Pa-s, cratonic survival potential improves slightly. Within this moderately viscous asthenosphere, cratonic roots of 10 times viscosity contrast (0.1, 10) experience $\sim 30 - 80\%$ areal reduction in roots and $\sim 40\%$ surface stretching (Fig. 8). With this viscosity combination also long term survival is not possible. With the increase of cratons' viscosity contrast, survival potential increases as the areal deformation of their roots and surface stretching decrease. If the cratons are 100 times more viscous (0.1, 100), areal reduction of the roots is restricted within $\sim 10\% - 30\%$ with negligible surface stretching. Indeed, this viscosity combination can potentially give rise to stable cratons that can survive for a long time (Fig. 6).

If the asthenosphere is strong, i.e., viscosity is in the order of 10^{21} Pa-s, cratons of even 10 times viscosity contrast (1, 10) undergo very small amount of deformation. Cratonic roots almost remain undeformed (only $\sim 5\%$ to $\sim 10\%$ areal reduction) while surface deformation is also restricted to within $\sim 10\%$ (Fig. 8). Stronger cratonic roots (1, 100) or (1, 1000) undergo even smaller deformation (Figs. 7, 8).

We have also calculated the final areal deformation of cratons at the present-day (Fig. 10a, Figs. S1, S2). As we keep on increasing the viscosity of asthenosphere and cratons, net deformation decreases. From the weakest model (0.01, 10) to the strongest model (1, 1000) final deformation follows two different almost linear trends of areal deformation of cratonic roots and surface deformation. This indicates that the intensity of deformation of the cratons increases as the viscosity of cratons and asthenosphere reduces.

4. Survival of cratons over ages

In this time-dependent study, we sought to understand the evolution and survival potential of cratons since 410 Ma. Because global plate reconstruction models do not go beyond 410 Ma, we are yet to develop time-dependent convection models that begin at the Archean. However, within the given limitations, our experiments produce results that are in agreement with Paul et al. (2019), who calculated the survival potential of cratonic roots (> 200 km) of different viscosity combinations from their instantaneous models using a scaling approach. Fig. 10b (same as Fig. 7b in Paul et al. (2019)) shows the survival time of cratons for different viscosity combinations of cratonic lithosphere and asthenosphere. Colored lines mark the range of inverse of non-dimensionalized strain-rates (INS) required for a cratonic root to survive within or beyond that time period. INS was calculated by taking the ratio of average normalized strain-rates within cratons having thickness more than 200 km to the average normalized strain-rates within oceanic lithosphere of thickness ranging from 0 to 72 km. Details of assumptions and limitations of the scaling approach are discussed in Paul et al. (2019). If INS of a cratonic root of certain viscosity combination falls below the green lines, which represent the INS of the Cambrian period (540 Ma), it is expected that the cratonic roots formed during Cambrian will be destroyed before they reach the present-day. Fig. 10b shows that the viscosity combination of 10^{19} Pa-s asthenosphere and 10 times viscous cratons

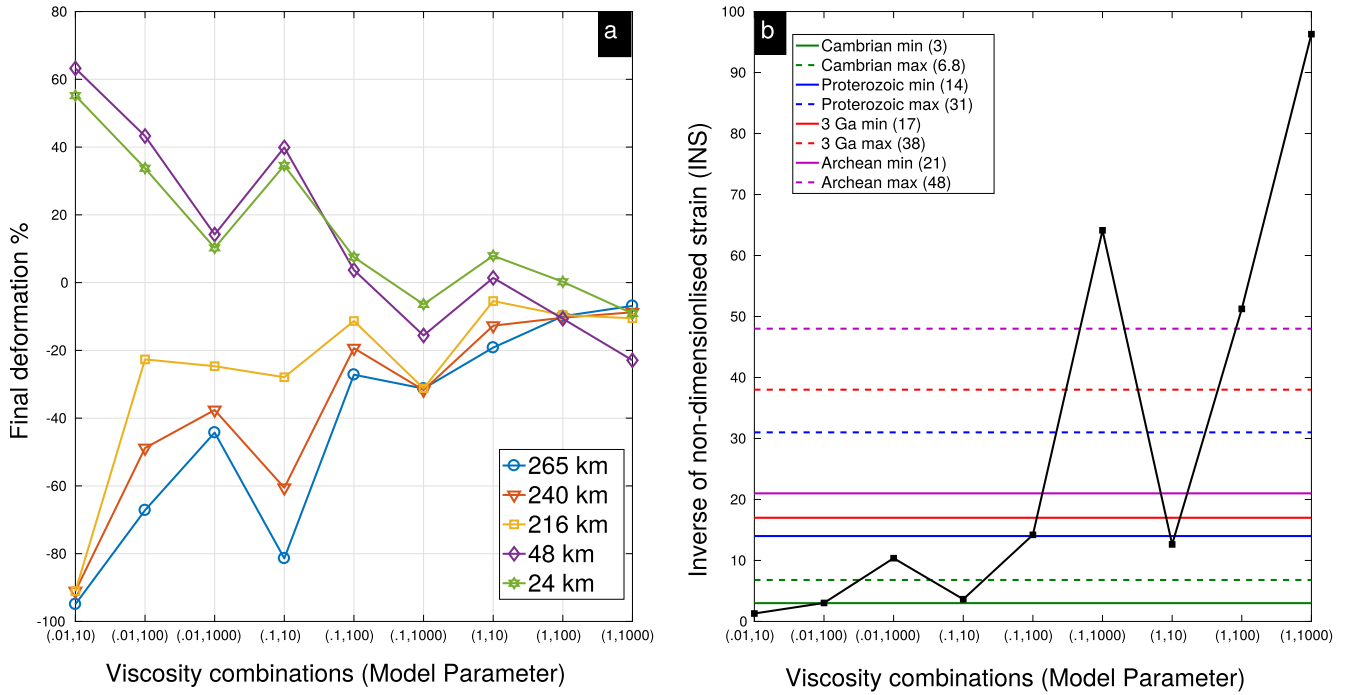


Fig. 10. (a) Final deformation of cratonic roots and near-surface stretching close to the present-day predicted from our models. Viscosity combination of each model is mentioned along the x-axis and the amount of deformation is mentioned along the y-axis. Different colors indicate different depths as mentioned in the legend. (b) Cratonic survival times estimated from scaling approach in instantaneous convection models (Fig. 7b of Paul et al. (2019)). The x-axis shows viscosity combination of the models. Horizontal colored lines specify the INS values for Cambrian, Proterozoic, Archean and at 3 Ga. Y-axis indicates INS values obtained from models with different viscosity combinations. Solid lines represent the INS values calculated using the age of oceanic plate as 180 Ma and the dashed lines represent the INS values calculated assuming that the oceanic plate starts to flatten due to convective shearing at 80 Ma (figure published in Paul et al., 2019). Model parameters in the x-axis are described in Table S1.

(0.01, 10) falls below the INS values of Cambrian, indicating that a craton originating during the Cambrian cannot survive till the present-day. In the present study also, we find that cratons with the said viscosity combination get destroyed within ~ 400 Myr (Figs. 3, 8, 10a).

For the models with viscosity combination of (0.01, 100) and (0.1, 10), the instantaneous results of Paul et al. (2019) predicted that cratonic roots formed during Cambrian (540 Ma) might marginally survive till the present-day. The present time-dependent study shows that with similar viscosity combination, cratonic roots are significantly deformed within 400 Myr and the roots of the smaller cratons such as Indian, Australian and Sao Francisco cratons, are completely destroyed. However, other large cratons have survived, although their intense deformation indicates that they may not be able to survive for another billion years (Figs. 5, 8, 10a).

As predicted by the earlier scaling method of Paul et al. (2019), increasing asthenosphere viscosity increases the chance of cratonic survival; near identical results are obtained in the present time-dependent study. The present study also shows that a model with viscosity combination of 10^{20} Pa-s asthenosphere and 100 times viscous cratons (0.1, 100) can potentially survive much longer than 410 Myrs, in spite of some notable deformation of cratonic roots and surface stretching (Fig. 6). This viscosity combination is probably the minimum requirement for a craton to survive for billions of years if they are only subjected to mantle shearing. It is to be noted that although the absolute viscosity of cratonic roots in models (0.01, 1000), (0.1, 100) and (1, 10) is similar, each of them undergoes different amount of deformation. Same is true for models having viscosity combination of (1, 100) and (0.1, 1000). Each of these models differs by ~ 10 – 20% at the final deformation stage, which confirms the role of asthenospheric viscosity in the survival of cratons.

5. Conclusion

The present study allows us to understand the control of asthenosphere and craton viscosity on the evolution of cratons. Our goal is to investigate the role of mantle flow in the long-term survival of cratons. This is the first attempt to address this issue by developing realistic spherical mantle convection models driven by reconstructed plate velocities. Earlier studies mostly used 2-D models to address this problem (Lenardic and Moresi, 1999; Lenardic et al., 2000, 2003; Sleep, 2003; O'Neill et al., 2008; Wang et al., 2014). There are a few regional 3-D spherical studies that have attempted to understand the problem of cratonic survival but they neither chose the real time location of the cratons nor did they use realistic (plate-reconstructed) velocities (Yoshida, 2010, 2012). Those studies placed high viscosity blocks inside a velocity field generated by thermal perturbation and studied their deformation. In our case, we have reconstructed the cratons' locations back in time and have forward-modeled mantle convection from 409 Ma to the present-day. Because we have imposed velocity boundary conditions obtained by finite rotation of the Euler poles (Matthews et al., 2016), cratons in our models evolve under realistic velocity field that causes deformation. Although, having density anomalies in the mantle would have been useful, the reconstructed density models do not go so far back in time.

As our models do not have lateral density variations and thickening of the lithosphere due to thermal cooling, we estimate only the minimum requirement of viscosity combinations of cratons and asthenosphere for the cratons to persist beyond 410 Myr if mantle shearing is the only destructive force. Lee et al. (2011) discussed several other potential reasons for the destruction of cratons. If all those processes work simultaneously, cratons may require even higher viscosities to resist deformation. The next level of challenge will be to replicate those geological phenomena (e.g. metasomatism, thermal cooling, varying cratonic thickness, tem-

perature dependent viscosity) in numerical modeling studies. Also, assigning different Rayleigh numbers for the mantle (Jaupart et al., 2007; Wang et al., 2015) might have some effect on the survival of cratons that could be taken up in future studies.

We find that interaction between the cratonic lithosphere and mantle shearing causes a significant amount of deformation underneath the cratons. This shearing is sufficient to recycle the lithospheric material if it is not strong enough. Asthenosphere viscosity surrounding the cratonic lithosphere is also quite important. If the viscosity of the asthenosphere drops, it can accommodate faster strain-rates. Hence, a very low viscosity asthenosphere surrounding the cratons is not desirable if cratons are to survive for a long time. We find that a minimum value of 10^{20} Pa-s is a good estimate of asthenospheric viscosity that can stabilize cratons.

It is quite obvious that the viscosity of the cratonic roots must play a very significant role in their survival. Our numerical models suggest that in the presence of moderately strong asthenosphere, cratonic roots 100 times more viscous than their surroundings can potentially survive for ~ 410 Myrs. Our predicted viscosity combinations of cratons and asthenosphere are in agreement with the earlier instantaneous mantle flow modeling results of Paul et al. (2019). We conclude that if mantle convection is the only force acting to destroy cratonic roots, cratons must be at least 100 times more viscous than the ambient layer and asthenosphere surrounding the cratonic roots should have the viscosity of 10^{20} Pa-s or more to achieve long-term survival.

Declaration of competing interest

We do not have any competing financial interests or personal relationships that could have appeared to influence the work reported in this paper.

Acknowledgement

We thank Adam Beall and Shijie Zhong for reviewing the manuscript and providing comments that considerably improved the quality of the manuscript. Convection code CitcomS-3.3.1 is maintained by Computational Infrastructure for Geodynamics (CIG). We thank Sabin Zahirovic, Dan Bower and Thorsten Becker for helping with GPlates reconstruction and CitcomS tracer handling. We also thank Clint Conrad for some insightful discussion. All models were run using a Cray XC40 system at the Supercomputer Education and Research Centre (SERC), IISc. Figures were produced using GMT 4.5.11 by P. Wessel and W.F. Smith and MATLAB 9.1 licensed at IISc.

Appendix A. Supplementary material

Supplementary material related to this article can be found online at <https://doi.org/10.1016/j.epsl.2019.115962>.

References

Artemieva, I., Mooney, W., 2002. On the relations between cratonic lithosphere thickness, plate motions, and basal drag. *Tectonophysics* 358 (1), 211–231.

Auer, L., Boschi, L., Becker, T., Nissen-Meyer, T., Giardini, D., 2014. Savani: a variable resolution whole-mantle model of anisotropic shear velocity variations based on multiple data sets. *J. Geophys. Res., Solid Earth* 119 (4), 3006–3034.

Becker, T., Boschi, L., 2002. A comparison of tomographic and geodynamic mantle models. *Geochem. Geophys. Geosyst.* 3 (1), <https://doi.org/10.1029/2001GC000168>.

Belousova, E., Kostitsyn, Y., Griffin, W.L., Begg, G.C., O'Reilly, S.Y., Pearson, N.J., 2010. The growth of the continental crust: constraints from zircon Hf-isotope data. *Lithos* 119 (3), 457–466.

Boyd, J.A., Müller, R.D., Gurnis, M., Torsvik, T.H., Clark, J.A., Turner, M., Ivey-Law, H., Watson, R.J., Cannon, J.S., 2011. Next-generation plate-tectonic reconstructions using GPlates. In: Keller, G., Bar, C. (Eds.), *Geoinformatics: Cyberinfrastructure for the Solid Earth Sciences*. Cambridge University Press, pp. 95–114.

Conrad, C.P., Lithgow-Bertelloni, C., 2006. Influence of continental roots and asthenosphere on plate-mantle coupling. *Geophys. Res. Lett.* 33 (L05), 312. <https://doi.org/10.1029/2005GL025621>.

Cooper, C., Lenardic, A., Moresi, L.N., 2004. The thermal structure of stable continental lithosphere within a dynamic mantle. *Earth Planet. Sci. Lett.* 222 (3), 807–817.

Dhuime, B., Hawkesworth, C.J., Cawood, P.A., Storey, C.D., 2012. A change in the geodynamics of continental growth 3 billion years ago. *Science* 335 (6074), 1334–1336.

Domeier, M., Torsvik, T.H., 2014. Plate tectonics in the late Paleozoic. *Geosci. Front.* 5 (3), 303–350.

Foley, S.F., 2008. Rejuvenation and erosion of the cratonic lithosphere. *Nat. Geosci.* 1 (8), 503. <https://doi.org/10.1038/ngeo261>.

Garber, J.M., Maurya, S., Hernandez, J.-A., Duncan, M.S., Zeng, L., Zhang, H.L., Faul, U., McCammon, C., Montagner, J.-P., Moresi, L., et al., 2018. Multidisciplinary constraints on the abundance of diamond and eclogite in the cratonic lithosphere. *Geochem. Geophys. Geosyst.* 19 (7), 2062–2086.

Ghosh, A., Becker, T.W., Zhong, S.J., 2010. Effects of lateral viscosity variations on the geoid. *Geophys. Res. Lett.* 37 (1). <https://doi.org/10.1029/2009GL040426>.

Ghosh, A., Becker, T.W., Humphreys, E.D., 2013. Dynamics of the North American continent. *Geophys. J. Int.* 194 (2), 651–669.

Ghosh, A., Thyagarajulu, G., Steinberger, B., 2017. The importance of upper mantle heterogeneity in generating the Indian Ocean geoid low. *Geophys. Res. Lett.* 44 (19), 9707–9715.

Gung, Y., Panning, M., Romanowicz, B., 2003. Global anisotropy and the thickness of continents. *Nature* 422 (6933), 707–711.

Gurnis, M., Turner, M., Zahirovic, S., DiCaprio, L., Spasojevic, S., Müller, R.D., Boyden, J., Seton, M., Manea, V.C., Bower, D.J., 2012. Plate tectonic reconstructions with continuously closing plates. *Comput. Geosci.* 38 (1), 35–42.

Hawkesworth, C., Kemp, A., 2006. Evolution of the continental crust. *Nature* 443 (7113), 811–817.

Hawkesworth, C., Cawood, P.A., Dhuime, B., Kemp, T.I., 2017. Earth's continental lithosphere through time. *Annu. Rev. Earth Planet. Sci.* 45 (1), 169–198.

Hoffman, P.F., 1988. United plates of America, the birth of a craton: early Proterozoic assembly and growth of Laurentia. *Annu. Rev. Earth Planet. Sci.* 16 (1), 543–603.

Humphreys, E.D., Schmandt, B., Bezada, M.J., Perry-Houts, J., 2015. Recent craton growth by slab stacking beneath Wyoming. *Earth Planet. Sci. Lett.* 429, 170–180.

Jaupart, C., Molnar, P., Cottrell, E., 2007. Instability of a chemically dense layer heated from below and overlain by a deep less viscous fluid. *J. Fluid Mech.* 572, 433–469.

Jordan, T., 1975. The continental tectosphere. *Rev. Geophys.* 13 (3), 1–12.

Jordan, T., 1978. Composition and development of the continental tectosphere. *Nature* 274 (5671), 544–548.

Kaban, M., Mooney, W., Petrunin, A., 2015. Cratonic root beneath North America shifted by basal drag from the convecting mantle. *Nat. Geosci.* 8 (10), 797–800.

Karato, S.-I., 2010. Rheology of the deep upper mantle and its implications for the preservation of the continental roots: a review. *Tectonophysics* 481 (1), 82–98.

King, S., 2005. Archean cratons and mantle dynamics. *Earth Planet. Sci. Lett.* 234 (1), 1–14.

Lee, C.-T.A., Lenardic, A., Cooper, C.M., Niu, F., Levander, A., 2005. The role of chemical boundary layers in regulating the thickness of continental and oceanic thermal boundary layers. *Earth Planet. Sci. Lett.* 230 (3), 379–395.

Lee, C.-T.A., Luffi, P., Chin, E.J., 2011. Building and destroying continental mantle. *Annu. Rev. Earth Planet. Sci.* 39, 59–90.

Lenardic, A., Moresi, L.N., 1999. Some thoughts on the stability of cratonic lithosphere: effects of buoyancy and viscosity. *J. Geophys. Res., Solid Earth* 104 (B6), 12747–12758.

Lenardic, A., Moresi, L.N., Mühlhaus, H., 2000. The role of mobile belts for the longevity of deep cratonic lithosphere: the crumple zone model. *Geophys. Res. Lett.* 27 (8), 1235–1238.

Lenardic, A., Moresi, L.N., Mühlhaus, H., 2003. Longevity and stability of cratonic lithosphere: insights from numerical simulations of coupled mantle convection and continental tectonics. *J. Geophys. Res., Solid Earth* 108 (B6). <https://doi.org/10.1029/2002JB001859>.

Matthews, K.J., Maloney, K.T., Zahirovic, S., Williams, S.E., Seton, M., Mueller, R.D., 2016. Global plate boundary evolution and kinematics since the late Paleozoic. *Glob. Planet. Change* 146, 226–250.

Müller, R.D., Seton, M., Zahirovic, S., Williams, S.E., Matthews, K.J., Wright, N.M., Shephard, G.E., Maloney, K.T., Barnett-Moore, N., Hosseinpour, M., et al., 2016. Ocean basin evolution and global-scale plate reorganization events since Pangea breakup. *Annu. Rev. Earth Planet. Sci.* 44, 107–138.

Nataf, H.-C., Ricard, Y., 1996. 3smac: an a priori tomographic model of the upper mantle based on geophysical modeling. *Phys. Earth Planet. Inter.* 95 (1–2), 101–122.

O'Neill, C., Lenardic, A., Griffin, W., O'Reilly, S., 2008. Dynamics of cratons in an evolving mantle. *Lithos* 102 (1), 12–24.

Paul, J., Ghosh, A., Conrad, C., 2019. Traction and strain rate at the base of the lithosphere: an insight into cratonic stability. *Geophys. J. Int.* 217 (2), 1024–1033.

- Pearson, D., Wittig, N., 2014. The formation and evolution of cratonic mantle lithosphere—evidence from mantle xenoliths. In: Turekian, K., Holland, H. (Eds.), *Treatise on Geochemistry*. Elsevier, New York, pp. 255–292.
- Pearson, D., Carlson, R., Shirey, S., Boyd, F., Nixon, P., 1995. Stabilisation of Archean lithospheric mantle: a Re–Os isotope study of peridotite xenoliths from the Kaapvaal craton. *Earth Planet. Sci. Lett.* 134 (3), 341–357.
- Polet, J., Anderson, D., 1995. Depth extent of cratons as inferred from tomographic studies. *Geology* 23 (3), 205–208.
- Pollack, H., 1986. Cratonization and thermal evolution of the mantle. *Earth Planet. Sci. Lett.* 80 (1–2), 175–182.
- Ritsema, J., Deuss, A.A., Van Heijst, H., Woodhouse, J., 2011. S40rts: a degree–40 shear-velocity model for the mantle from new Rayleigh wave dispersion, teleseismic traveltimes and normal-mode splitting function measurements. *Geophys. J. Int.* 184 (3), 1223–1236.
- Rudnick, R., McDonough, W., O'Connell, R., 1998. Thermal structure, thickness and composition of continental lithosphere. *Chem. Geol.* 145 (3), 395–411.
- Simmons, N.A., Forte, A.M., Boschi, L., Grand, S.P., 2010. Gypsum: a joint tomographic model of mantle density and seismic wave speeds. *J. Geophys. Res., Solid Earth* 115. <https://doi.org/10.1029/2010JB007631>.
- Sleep, N.H., 2003. Survival of Archean cratonic lithosphere. *J. Geophys. Res., Solid Earth* 108 (B6). <https://doi.org/10.1029/2002JB001859>.
- Wang, H., van Hunen, J., Pearson, D.G., Allen, M.B., 2014. Craton stability and longevity: the roles of composition-dependent rheology and buoyancy. *Earth Planet. Sci. Lett.* 391, 224–233.
- Wang, Y., Huang, J., Zhong, S., 2015. Episodic and multistaged gravitational instability of cratonic lithosphere and its implications for reactivation of the North China craton. *Geochem. Geophys. Geosyst.* 16 (3), 815–833.
- Yoshida, M., 2010. Preliminary three-dimensional model of mantle convection with deformable, mobile continental lithosphere. *Earth Planet. Sci. Lett.* 295 (1), 205–218.
- Yoshida, M., 2012. Dynamic role of the rheological contrast between cratonic and oceanic lithospheres in the longevity of cratonic lithosphere: a three-dimensional numerical study. *Tectonophysics* 532, 156–166.
- Zhang, N., Zhong, S., Leng, W., Li, Z.-X., 2010. A model for the evolution of the earth's mantle structure since the early Paleozoic. *J. Geophys. Res., Solid Earth* 115 (B6). <https://doi.org/10.1029/2009JB006896>.
- Zhong, S., Zuber, M., Moresi, L.N., Gurnis, M., 2000. Role of temperature-dependent viscosity and surface plates in spherical shell models of mantle convection. *J. Geophys. Res., Solid Earth* 105 (B5), 11063–11082.
- Zhu, R., Xu, Y., Zhu, G., Zhang, H., Xia, Q., Zheng, T., 2012. Destruction of the North China craton. *Sci. China Earth Sci.* 55 (10), 1565–1587.